Carbohydrate Polymers 196 (2018) 254–261

Contents lists available at ScienceDirect

Carbohydrate Polymers

journal homepage: www.elsevier.com/locate/carbpol

Polybutylene succinate/cellulose nanocrystals: Role of phthalic anhydride in squeeze oriented bionanocomposites

Xuzhen Zhang, Xiuhua Wang*

The Key Laboratory of Advanced Textile Materials and Manufacturing Technology of Ministry of Education, College of Materials and Textiles, National Engineering Lab for Textile Fiber Materials & Processing Technology, Zhejiang Sci-Tech University, China

ARTICLE INFO

Keywords:
Cellulose nanocrystal
Poly(butylene succinate)
Phthalic anhydride
Squeeze treatment
Crystallization
Composite

ABSTRACT

In order to reduce agglomerations and improve the compatibility of poly(butylenes succinate)/cellulose nanocrystals (PBS/CNC) composite, phthalic anhydride was introduced during the preparation of composite via melt blending. The composites were then suffered by squeezing treatment in a two-roll milling equipment at a given temperature. In order to investigate reaction mechanism among PBS, CNC and phthalic anhydride, PBS/CNC composites were separated and then tested via FTIR and UV–vis spectrophotometer. During reactive blending, phthalic anhydride selectively reacts with CNC, at an effective grafting ratio of 0.0196, which is confirmed by titration results. Before squeezing, the crystallinity of PBS in composites are increased but the mechanical properties of composites are weakened with increasing phthalic anhydride content, which is ascribed to the plasticizing effect of phthalic anhydride. After squeeze treatment at an extension ratio of 6, the tensile strength of PBS/PA/CNC(100/2/3) is dramatically increased from 35.2 MPa to 136 MPa. WAXD results show that PBS crystal type has little change but the crystallinity is sharply increased after orientation, which mostly contributes to the improvement of mechanical properties for PBS/CNC composites.

1. Introduction

Nowadays, biodegradable composites have been investigated and considered as an ideal type of product in order to replace nondegradable petroleum based materials (Jonoobi, Harun, Mathew, & Oksman, 2010; Kowalczyk, Piorkowska, Kulpinski, & Pracella, 2011; Petera et al., 2015; Sharifian, 2011; Zare, Lakouraj, & Mohseni, 2014; Zhang et al., 2015). Poly(butylene succinate), short for PBS, is one of the most suitable matrix materials for such biocomposites because of its relatively low cost, processibility and eco-friendly nature (Totaro et al., 2016). However, some certain applications of PBS are limited by its drawbacks in mechanical properties (Pérezcamargo et al., 2017). Although its flexibility and elongation at break are comparable to poly (ethylene terephthalate), one major disadvantage of PBS is its low tensile strength and elastic modulus (Li, Fu, Wang, & Zeng, 2017). Therefore, it is essential to find appropriate fillers to increase the strength of PBS in order to expand its application.

Cellulose nanocrystals (CNC) have aroused considerable attention due to their valuable properties, such as biodegradability, light weight, nano-scale effects, low cost, high specific strength and modulus (138 GPa of Young's modulus and 1.7 GPa of tensile strength), unique morphology, and relatively reactive surface (Azouz, Ramires, Fonteyne, Kissi, & Dufresne, 2012; Habibi et al., 2008; Lin, Huang, & Dufresne, 2012). CNC can be fabricated by strong acid or enzymatic hydrolysis, mechanical refining, ionic liquid treatment, subcritical water hydrolysis, oxidation method and combined processes from natural sources, having unique polymorph of cellulose (cellulose I) (Dhar, Bhasney, Kumar, & Katiyar, 2016; Mariano, Kissi, & Dufresne, 2014; Trache et al., 2016; Trache, Hussin, Haafiz, & Thakur, 2017). They have been widely studied as reinforcing agents in different kinds of nanocomposites, such as poly(e-caprolactone) (Stroganov et al., 2015), PLA (Bagheriasl, Carreau, Riedl, Dubois, & Hamad, 2016; Salmieri et al., 2014), chitosan hydrogel (Zhou, Fu, Zhang, Zhan, & Levit, 2014), PBS (Joy et al., 2017) and polystyrene (Huan, Bai, Liu, & Han, 2015; Zhang et al., 2013), etc. CNC presents obvious hydrophilicity because of a large amount of hydroxyl groups on their surface, which limits the compatibility between hydrophilic CNC and a hydrophobic polymeric matrix (Bagheriasl et al., 2016; Habibi, Lucia, & Rojas, 2010; Morandi, Heath, & Thielemans, 2009). Therefore, there are two challenges to overcome in the preparation of nanocomposites reinforced by CNC: the agglomeration tendency and the poor compatibility with nonpolar materials.

There are a large number of reactive hydroxyl groups on the surface of CNC, which can react with different active groups, such as carboxyl, epoxy, and siloxane, etc. In order to improve the thermal stability and

* Corresponding author at: No. 928, Second Avenue, Xiasha District, Hangzhou, 310018, China.
E-mail address: wxiuhua@126.com (X. Wang).

https://doi.org/10.1016/j.carbpol.2018.04.124
Received 9 November 2017; Received in revised form 17 April 2018; Accepted 30 April 2018
Available online 17 May 2018
0144-8617/

hydrophobicity of CNC, different chemical and physical modification strategies have been attempted (Eyley & Thielemans, 2014), such as solubilization using a third component as compatibilizer (Pracella, Haque, & Puglia, 2014), oxidation (Shimizu, Saito, & Isogai, 2014), polymer grafting (Goffin et al., 2011; Ljungberg et al., 2005), etc. The resulting nanocrystals show good dispersion abilities in organic solvents and excellent thermal stability. The goal of these methods was to introduce hydrophobic groups on the surface of the CNC to replace the hydrophilic hydroxyl groups.

Esterification, a type of chemical modification often used to reduce the polarity, functions by replacing the hydroxyl groups of cellulose with less hydrophilic agents (Li et al., 2017). Jonoobi, Mathew, Abdi, Makinejad, and Oksman (2012) reported that acetylated cellulose nanocrystals (ACNC) exhibited reduced polarity with virgin CNC with a degree of substitution (DS) values of 1.07. Zhang and Zhang (2016) prepared poly(butylene succinate) grafted CNC (PBS-*g*-CNC) through in situ polymerization. CNC has homogenous dispersion in composites and contributes to the mechanical properties of composites, even though PBS component in composites show lower molecular weight than virgin PBS. In our previous study, phthalic anhydride was added into PBSA/CNC composites to improve the compatibility between CNC and PBSA matrix. Both dispersion of CNC and modulus of PBSA/CNC composites are improved after the addition of phthalic anhydride (Zhang & Zhang, 2015). CNC modified by esterification show potential application as compatible reinforcement and nanofillers in nanocomposite production (Xu et al., 2016; Zhang, Ma, & Zhang, 2016), while esterification did not effectively improve the nanocomposite properties, as expected, due to the random arrangement of CNC in composites.

In this study, PBS/CNC composites was melt blending modified by phthalic anhydride to improve dispersion of CNC and interfacial adhesion between CNC and PBS matrix. The derivative was then squeezed to sheets with a given extension ratio in a double-roller milling device. The reaction mechanism between phthalic anhydride and CNC was investigated via FTIR method by separating composites with certain organic solvents. In addition, the microstructure of CNC, morphological characterization, thermal properties, mechanical properties and crystallization behavior of PBS/CNC composites were investigated in detail. The good compatibility of oriented PBS/CNC composite is expected to have potential in biomaterials or packaging applications.

2. Experimental

2.1. Materials

PBS (Bionolle 1001MD) was produced by Showa Denko Group (Japan) with M_n of 8.8×10^4 g/mol and polymer dispersity index (PDI) of 2.2. Microcrystalline cellulose (MCC) and phthalic anhydride were purchased from Sinopharm Chemical Reagent Co., Ltd. (China). CNC with length of 100–250 nm and diameter of 15–30 nm was extracted from MCC in sulfuric acid solution with the same method we used in previous study (Zhang & Zhang, 2016). The PBS pellets were dried in a vacuum oven at 60 °C for 48 h before use.

2.2. Preparation and separation of PBS/PA/CNC composites

PBS/PA/CNC composites were prepared using a Haake rheometer at a rotor speed of 60 rpm and 135 °C for 10 min, and compression molded for 10 min at 140 °C to get sheets with the thickness of 1 mm and 3 mm for measurements. PBS/CNC composites without phthalic anhydride were also prepared as contrast samples (Scheme 1).

In order to investigated the reaction among phthalic anhydride, CNC and PBS, 2 g prepared PBS/PA/CNC(100/1/3) composite was dissolved in chloroform and stirred for 24 h at room temperature. A transparent suspension (Suspension I) and some insoluble fraction (Insoluble fraction I) were obtained from the mixture suspension. Suspension I was washed with hot water for 3 times and precipitated with methanol to obtain Fraction I. To remove residual polymer, Insoluble fraction I was washed with chloroform for 3 times, and then separated with hot methylbenzene to get a solution and Insoluble fraction II. Like the treatment of Insoluble fraction I, Insoluble fraction II was also washed with hot methylbenzene for 3 times to obtain Fraction II. While the solution derived from Insoluble fraction I was simply dried to obtain Fraction III. The procedure details of separation are presented in Scheme 2. All separated fractions were weighted after dried in vacuum oven, and responding yield is 1.91, 0.07 and 0.005 g for Fraction I, II, III, respectively. PBS/PA/CNC(100/3/3) composite was also separated with the same procedures.

2.3. Preparation of oriented PBS/PA/CNC composites

Oriented PBS/PA/CNC composite sheets were prepared through rolling squeezing PBS/PA/CNC composite sheets with a thickness of 3 mm using a double roller mixing mill device (Yiyang Rubber & Plastic Machinery Group, China). All composite sheets had been dried in vacuum oven overnight. The treatment was conducted under 85 °C at a rolling speed of 85 rpm. Gap between two rollers was set as 1 mm and 0.5 mm, thus the extension ratio of PBS/PA/CNC composite sheets reached 3 and 6 times, respectively.

2.4. Charactorization

Infrared spectra were obtained by using a Spectrum 100 Fourier transform infrared spectra (FTIR) Spectrometer (Perkin Elmer, USA). An ultra-violet visible spectrophotometer (Perkin-Elmer Lambda, USA) was used to characterize the absorption properties of separated samples from PBS/PA/CNC composites. The state of dispersion of CNC samples was examined using a Transmission electron microscope (Hitachi, Japan) at 100KV. Morphology of PBS/PA/CNC composites and dispersion of CNC in composites were investigated on a SEM device (Nova NanoSEM, FEI Cor., USA). Before observation, all samples were freeze fractured by immersing intoliquid nitrogen and then sputter coated with gold. A drop of the diluted CNC suspension was deposited onto carbon-coated grids and allowed to dry at room temperature. The sample was negatively stained with a 2% uranyl acetate aqueous solution for several minutes prior to test. WAXD diffraction experiments were performed on a D/max-200/PC X-ray generator (Rigaku Cor., Japan) operated at 40 kV and 20 mA with Cu-Kα radiation ($\lambda = 0.154$ nm) at a scanning rate of 4°/min.

The tensile properties and flexural properties were measured using a universal test machine (SANS, MTS Systems Cor., USA). Tensile properties was tested at a crosshead speed of 20 mm min^{-1}, following ASTM D882-10. Dumbbell samples were prepared by cutting composites sheets into 75 mm in length, 1 mm in thickness, and 4 mm in width. Notched Izod impact strength was tested using a Ray-Ran universal Pendulum Impact Tester according to ASTM D256. The dimension of the samples for impact and flexural testing was $63.5 \times 12.7 \times 3$ mm^3. All samples were kept at 23 °C, 50% humidity for 24 h before testing.

Crystallinity and melting behavior of PBS composites were characterized using a DSC (Q2000, TA Instruments) at 20 °C/min in nitrogen. A sample was heated from −50 to 200 °C to eliminate previous thermal history, then cooled down to −50 °C, and finally heated to 200 °C.

3. Results and discussion

3.1. Morphology analysis of cellulose nanocrystals and composites

TEM image and size distribution of the freeze-drying CNC are shown in Fig. 1. Image-Pro Plus software was employed to calculate and analyze size of CNC based on TEM images. In the images, it is evident that rod-like morphology and nano-scale of CNC were preserved. The diameter and length of cellulose nanocrystals are summarized in

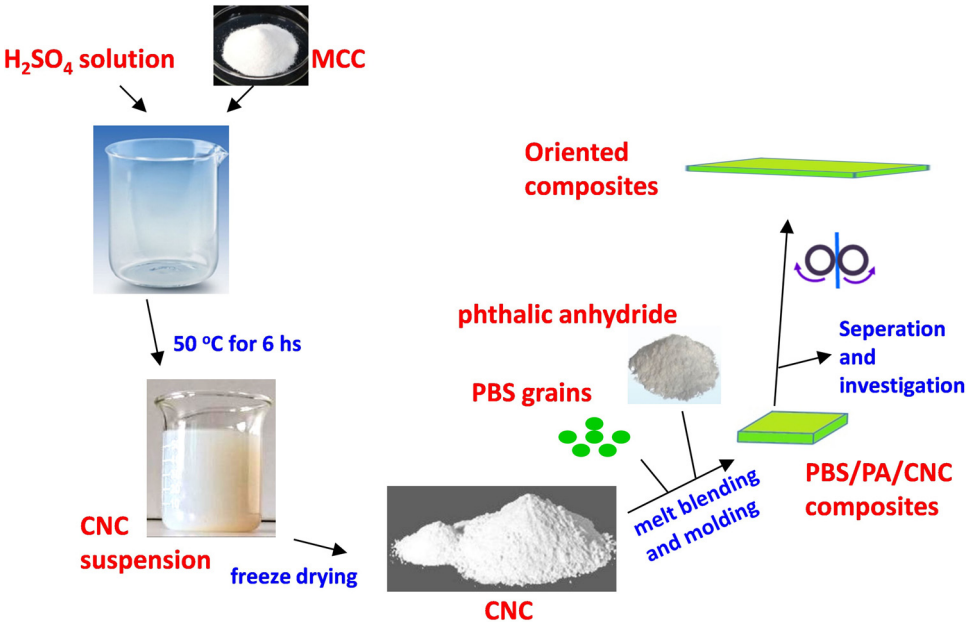

Scheme 1. Peparation of oriented PBS/PA/CNC composites.

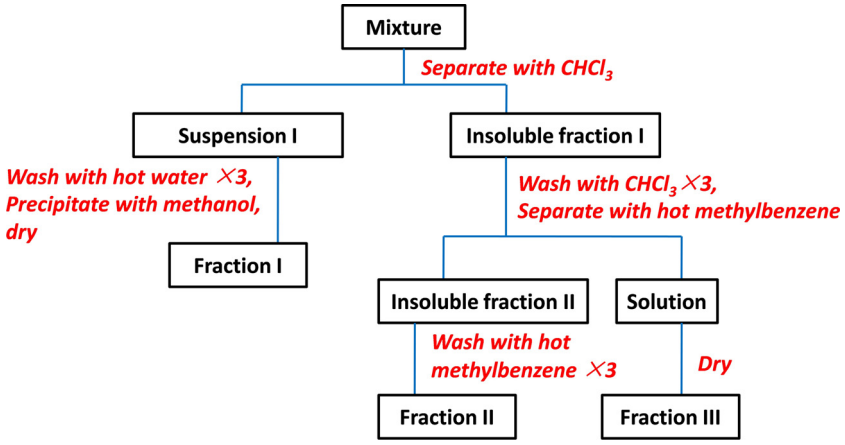

Scheme 2. Extraction of the substances from PBS/PA/CNC(100/1/3) composite.

Fig. 1(a) and (b), respectively. Single CNC was observed with a diameter of 27 ± 10 nm and a length of 400 ± 150 nm, which is similar to the results of other CNC researches (Pranger & Tannenbaum, 2008).

Fig. 2 shows section morphology of virgin PBS and its composites. As shown in Fig. 2(a) and (b), CNC exhibits some aggregation in PBS matrix. While after the addition of phthalic anhydride, CNC has a homogenous disperse in both PBS/PA/CNC(100/3/3) composite and PBS/PA/CNC(100/4/3) composite, revealing a good compatibilizing effect of phthalic anhydride between CNC and PBS.

3.2. Spectrograms of separation components in PBS/PA/CNC

Fig. 3 shows FTIR and UV-visual spectra of separated samples from PBS/PA/CNC (100/1/3) composite. Spectra of virgin PBS, CNC and

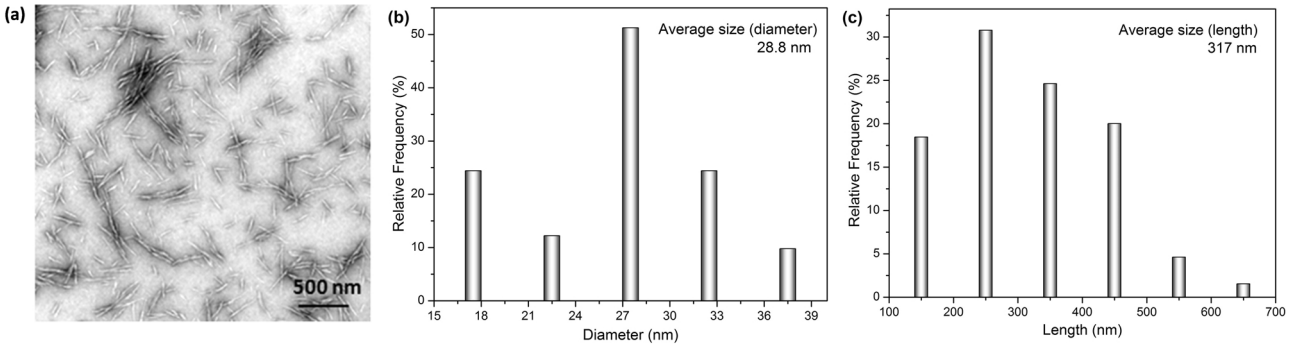

Fig. 1. (a) TEM image of CNC sample obtained from 6 h MCC acid hydrolysis and its size distribution of (b) diameter and (c) length.

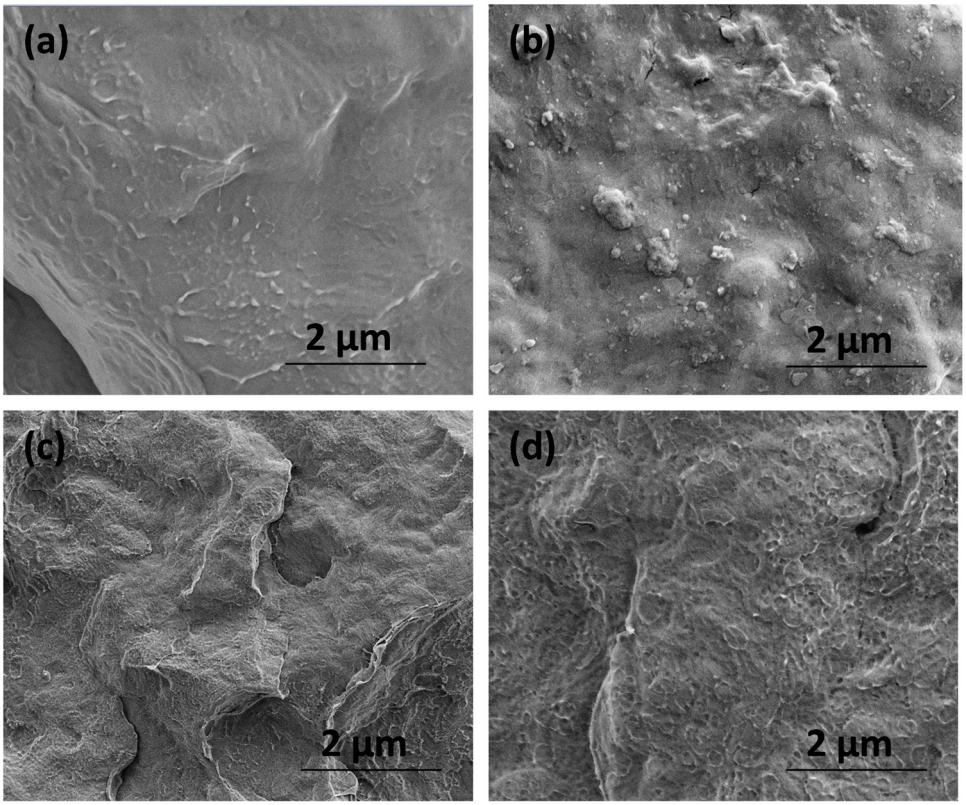

Fig. 2. SEM images of (a) virgin PBS, (b) PBS/PA/CNC(100/1/3), (c) PBS/PA/CNC(100/3/3) and (d) PBS/PA/CNC(100/4/3).

phthalic anhydride are also presented as contrasts. Compared with the spectrum of PBS, Fraction I has the same peaks, showing the same chemical structure as PBS (Fig. 3(a)). For unmodified CNC, the absorption bands at 3376 and 2897 cm^{-1} are attributed to cellulose vibration. Fraction II has similar peaks except for a band around 1759 cm^{-1}, which is assigned to the bond in phenylene agent of phthalic anhydride (Yu, Asai, & Sumita, 2000). As a result, Fraction II is mainly CNC with a few amount of phthalic anhydride component. Considering thorough washing treatment to remove phthalic anhydride from Fraction II, PA-CNC should be achieved through the reaction between anhydride agents and hydroxyl agents. Fraction III can be confirmed as phthalic anhydride by comparing its spectrum and that of virgin phthalic anhydride.

In addition, UV-visual spectra of separated samples from PBS/PA/CNC (100/1/3) composite is used to confirm the results of FTIR analysis (Fig. 3(b)). PBS, CNC and Fraction I show no sign of absorption in a wavelength range of 200–310 nm, indicating that Fraction I is short of UV absorption agent. While phthalic anhydride and Fraction III curves exhibit bands located 230 and 280 nm, respectively. These bands are all related to phenylene agents (Flego, Kiricsi, Perego, & Bellussi, 1995). Fraction II also have such two peaks as phthalic anhydride, but the peaks are much weaker and the curve is more closed to that of CNC, showing a structure combing CNC and phthalic anhydride. According to the comprehensive results of FTIR and UV–vis spectra, Fraction I, II, III could be confirmed as PBS, CNC-PA, phthalic anhydride, respectively.

Neutralization titration after saponification reaction was used to investigate the graft ratio of PA-CNC from PBS/PA/CNC(100/1/3) and PBS/PA/CNC(100/3/3) according to the method in our previous work (Zhang et al., 2016), and the results are shown in Table 1. Phthalic anhydride agent contents in CNC-PA increase from 1.73 to 1.96% with composition ratio of phthalic anhydride and CNC increasing from 1:3 to 3:3, and the corresponding graft ratio of CNC-PA is 0.0173 and 0.0196, respectively. The result show that phthalic anhydride is over loaded in PBS/PA/CNC(100/3/3) composite.

3.3. Thermal and mechanical properties of PBS/PA/CNC

PBS is a typical semicrystalline polymer. Its mechanical and thermal resistance properties are greatly dependent on the solid-state morphology and high crystallinity. Accordingly, it is very important to study the influence of CNC and phthalic anhydride on the crystallization of matrix polymers in composites. Fig. 3(c) shows second heating run thermograms of PBS/PA/CNC with a variety of phthalic anhydride contents. As shown in Fig. 3(c), one exothermic peak located around 113 °C can be observed in all composites curves. The melting point of composites has little change but the incipient melting temperature is decreased from 105 to 98 °C with increasing phthalic anhydride content, revealing that the addition of phthalic anhydride reduce the integrity of PBS crystal. The WAXD patterns of PBS/PA/CNC composites were investigated to obtain insight into crystallinity, as shown in Fig. 3(d). The crystal unit cell of PBS is monoclinic and the diffraction peaks from (020), (021) and (110) are observed at Bragg angles of 19.5°, 21.5° and 22.5°, respectively. The diffraction peaks location of PBS has little change with PA:CNC ratio increasing from 0:3 to 3:3, indicating that crystalform of PBS is remained during the modification process. The crystallinity of PBS component in composites, calculated from the analyze results of Jade, is increasing from 25% of virgin PBS to 45% of PBS/PA/CNC (100/3/3). Similar crystallinity increase also appeared in our previous work about poly(butylene succinate-*co*-butylene adipate)/cellulose nanocrystal composites modified with phthalic anhydride (Zhang & Zhang, 2015). Considering the reduction of crystal integrity based on the DSC results above, the number of crystallization point should be increased with increasing phthalic anhydride content.

PBS is known as a ductile polymer with a high elongation at break, low tensile strength and low modulus (Wan & Chen, 2013). As shown in Table 2 and Fig. 4, tensile strength, flexural strength, flexural modulus all increase with the incorporation of CNC and phthalic anhydride, which is related to high modulus of CNC and an compatibilizing effect

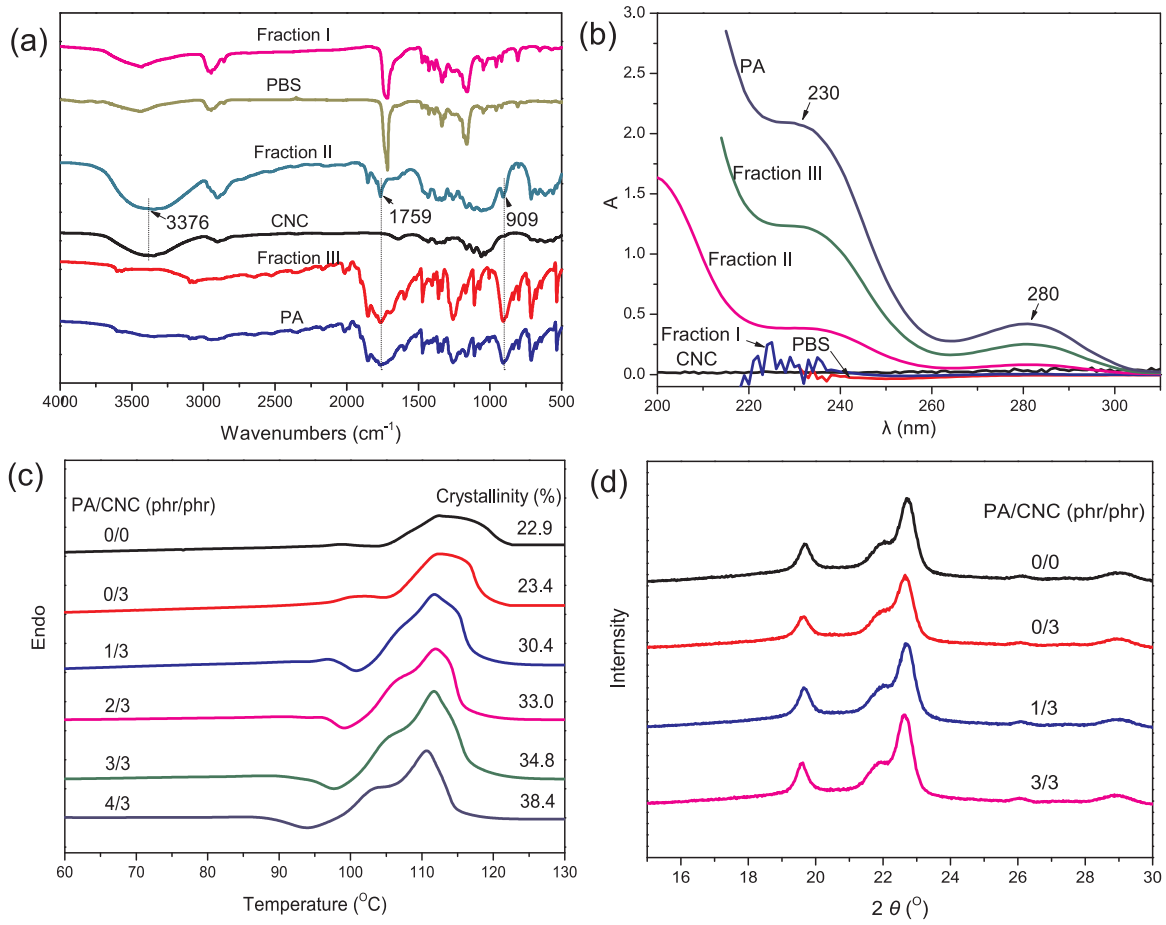

Fig. 3. (a) FTIR and (b) UV-visual spectra of separated samples from PBS/PA/CNC (100/1/3) composite; (c) DSC heating traces and (d) WAXD patterns of PBS/PA/CNC composites with increasing PA content.

Table 1
Graft ratio of PA-CNC obtained from neutralization titration.

PA/CNC(phr/phr)	PA agent content (%)	Graft ratio
Control	0	0
1/3	1.73	0.0173
3/3	1.96	0.0196

Table 2
Mechanical parameters of PBS/PA/CNC composites.

PA/CNC(phr/phr)	σ_b (MPa)	ε_b (%)	Flexural strength (MPa)	Flexural modulus (MPa)	Impact strength (J/m)
0/0	22.8	81.6	30.1	473	112
0/3	34.5	91.8	31.7	584	112
1/3	35.2	83.2	32.9	649	162
2/3	33.4	77.7	31.2	624	111
3/3	30.0	72.2	28.6	499	98
4/3	27.7	73.0	27.4	507	83

of phthalic anhydride (Zhang & Zhang, 2016). However, the mechanical properties of PBS/CNC composites decrease with increasing phthalic anhydride content, which should be ascribed to the reinforcement of CNC and plasticizing effect of redundant phthalic anhydride on PBS/PA/CNC composites (Trabelsi-Souissi, Oturan, Bellakhal, & Oturan, 2011). The impact strength evaluation is an important tool to study the fracture toughness of polymer composites. Impact strength of PBS is also compared with that of other composites in Table 2. The notched izod impact strength and elongation at break of the PBS composites are significantly affected by phthalic anhydride. When the CNC content is 3 phr, the impact strength of PBS/CNC decreases from 162 to 83 J/m with increasing phthalic anhydride content from 1 to 3 phr, which is much lower than that of PBS based composites in other researches (Ray, Okamoto, & Okamoto, 2003). The decrease of strength and modulus with phthalic anhydride is reasonable because phthalic anhydride can lead to some incomplete PBS crystals in polymer matrix due to the plasticizing effect, which will weaken the strength of composites.

3.4. Mechanical properties of oriented PBA/PA/CNC composites

In order to investigate the mechanical properties of PBS/PA/CNC composites in film or plate application, the obtained PBS/PA/CNC composites were then subjected to extension process. Tensile strength of PBS/PA/CNC composites with a variety of phthalic anhydride contents after 3 or 6 times extension are shown in Fig. 5(a), and the detailed mechanical parameter are summarized in Table 3.

As shown in Fig. 5, tensile strength of virgin PBS is 22.8 MPa, which increases to 55.5 and 92.2 MPa after 3 and 6 times extension ratio, respectively. Similar to virgin PBS, PBS/CNC composites modified by phthalic anhydride also show sharply increase in their tensile strength. For example, tensile strength of PBS/PA/CNC(100/1/3) increases to 58.9 and 132 MPa with 3 and 6 times extension ratio, which is 167% and 375% of that of the composite before extension respectively. This tendency is even more obvious with increasing phthalic anhydride content under 3 phr. While elongation at break of composites after extension show some decrease to a range of 18.6–41.3%, which should

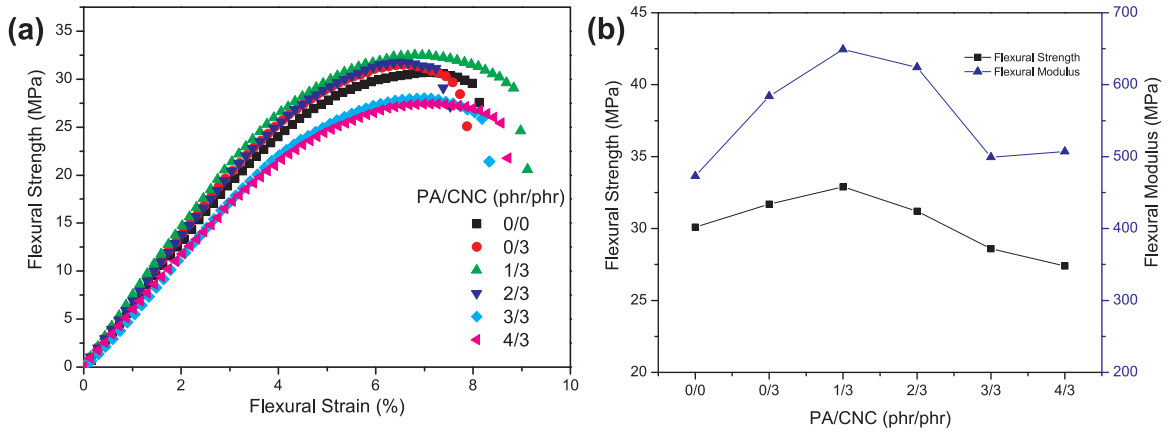

Fig. 4. Flexural properties of PBS/PA/CNC composites.

not affect composite materials for plastic application. The increased tensile strength of PBS/CNC might be ascribed to the following reasons: (a) The planar orientation of PBS macromoleculars may occur during the extension process. (b) The planar ordered arrangement of CNC in composites may occur during the extension process. (c) Orientation-induced crystallization could be increased by the oriented PBS macromoleculars, which should promote crystallinity and tensile strength. The plasticizing effect of phthalic anhydride contributes to the arrangement of PBS macromoleculars, while overloaded phthalic anhydride is detrimental to tensile strength of composites.

WAXD method was employed to investigated crystallization properties of PBS/PA/CNC composites before and after extension, the patterns and crystallicity histogram are shown as Fig. 5(b, c). In the pattern of PBS/PA/CNC(100/1/3) composite, the peak at 22.5° is sharply enhanced by extension process. Distinguish with peak intensity, the location of peaks has little change after extension, showing that PBS

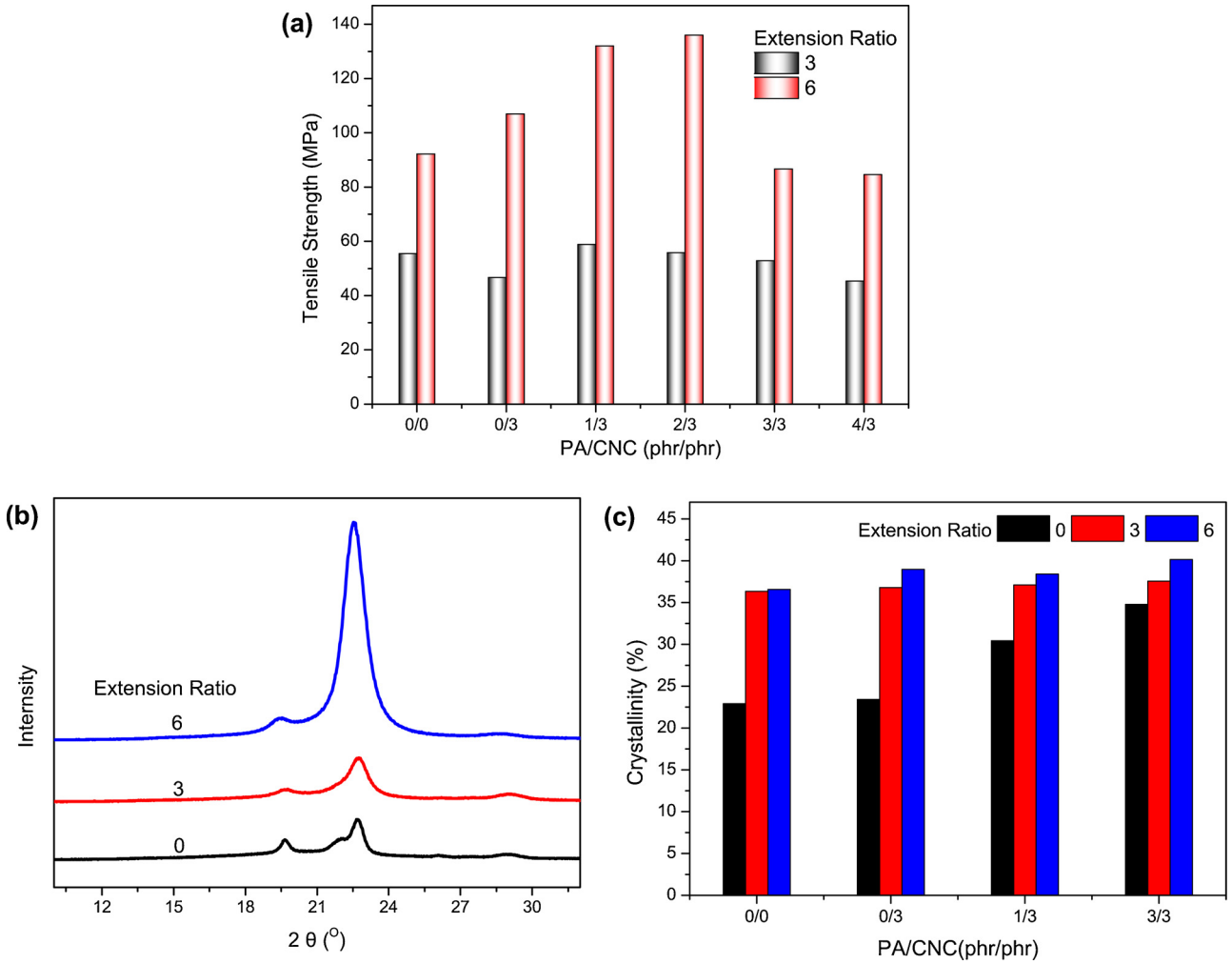

Fig. 5. (a)Tensile strength of oriented PBS/PA/CNC composites; (b) WAXD patterns of PBS/PA/CNC(100/1/3) composites and (c) the crystallinity histogram of oriented PBS/PA/CNC composites with increasing PA content.

Table 3
Mechanical parameters of oriented PBS/PA/CNC composites.

PA/CNC (3)[a](phr/phr)	σ_b (MPa)	ε_b (%)	PA/CNC (6)[a] (phr/phr)	σ_b (MPa)	ε_b (%)
0/0	55.5	41.3	0/0	92.2	27.2
0/3	46.7	67.6	0/3	107	28.6
1/3	58.9	89.7	1/3	132	23.9
2/3	55.8	47.0	2/3	136	22.6
3/3	52.9	27.6	3/3	86.7	14.7
4/3	45.4	22.3	4/3	84.6	18.6

[a] PA/CNC (3) refers to composites extended at a ratio of 3 and PA/CNC (6) refers to composites extended at a ratio of 6.

polymorph is maintained. In Fig. 5(c), crystallinity of all samples increase after 3 or 6 times extension, confirming the orientation-induced crystallization effect discussed above. That is the main reason why tensile strength increases sharply after extension. In addition, with increasing phthalic anhydride content, PBS/PA/CNC(100/1/3) composite after extension shows higher crysallinity, which should be related to easier disentanglement of PBS macromoleculars plasticized by phthalic anhydride.

4. Conclusions

Cellulose nanocrystal (CNC), with a diameter of 27 ± 10 nm and a length of 400 ± 150 nm, was prepared by hydrolyzing microcrystalline cellulose in sulfuric acid. A novel polybutylene succinate/cellulose nanocrystal (PBS/CNC) composite modified by phthalic anhydride to improve compatibility was prepared via simple melting blending, which is followed by a squeeze extension treatment on a double roller mixing mill device. Reaction mechanism among PBS, CNC and phthalic anhydride was investigated through FT-IR and UV-visual spectra of components separated from PBS/PA/CNC(100/1/3) composite. During the blending, phthalic anhydride selectively reacted with CNC at a graft ratio of 0.0173.

1. As convinced by DSC and WAXD results, the incipient melting temperature of PBS/CNC composites is decreased with increasing phthalic anhydride content mostly due to the plasticizing effect but the melt point has little change. Meanwhile, crystallinity of composites is increased with increasing phthalic anhydride content, showing that PBS component has more but smaller crystals after the addition of phthalic anhydride. Tensile strength, flexural strength, flexural modulus all increase with the incorporation of CNC, but decrease with increasing phthalic anhydride content, which should be ascribed to the reinforcement of CNC and plasticizing effect of redundant phthalic anhydride on PBS/PA/CNC composites.
2. Tensile strength of pristine PBS, PBS/CNC composites and PBS/PA/CNC composites is all significantly increased by extension treatment, and this tendency is more obvious with increasing phthalic anhydride content under 3 phr.
3. WAXD results show that crystal form of PBS component has little change but the crystallinity of composites is sharply increased after extension treatment. The enhanced crystallinity can be considered as the mean reason leading to the improvement of mechanical properties. With increasing phthalic anhydride content, PBS/PA/CNC(100/1/3) composite after extension shows higher crysallinity, which should be related to easier disentanglement of PBS macromoleculars plasticized by phthalic anhydride.

Acknowledgements

The authors gratefully acknowledge The National Key Research and Development Program of China (No. 2016YFB0302900), Zhejiang Provincial Natural Science Foundation of China (No. LQ18E030010) and Green Manufacturing System Integration Project (No. Z135060009002) for the financial support.

References

Azouz, K. B., Ramires, E. C., Fonteyne, W. V. D., Kissi, N. E., & Dufresne, A. (2012). Simple method for the melt extrusion of a cellulose nanocrystal reinforced hydrophobic polymer. *ACS Macro Letters, 1*(1), 236–240.
Bagheriasl, D., Carreau, P. J., Riedl, B., Dubois, C., & Hamad, W. Y. (2016). Shear rheology of polylactide (PLA)–cellulose nanocrystal (CNC) nanocomposites. *Cellulose, 23*(3), 1885–1897.
Dhar, P., Bhasney, S. M., Kumar, A., & Katiyar, V. (2016). Acid functionalized cellulose nanocrystals and its effect on mechanical, thermal, crystallization and surfaces properties of poly (lactic acid) bionanocomposites films: A comprehensive study. *Polymer, 101*, 75–92.
Eyley, S., & Thielemans, W. (2014). Surface modification of cellulose nanocrystals. *Nanoscale, 6*(14), 7764–7779.
Flego, C., Kiricsi, I., Perego, C., & Bellussi, G. (1995). Adsorption of propene, benzene, their mixtures and cumene on H-beta zeolites studied by IR and UV–vis spectroscopy. *Studies in Surface Science & Catalysis, 94*(06), 405–412.
Goffin, A. L., Raquez, J. M., Duquesne, E., Siqueira, G., Habibi, Y., Dufresne, A., et al. (2011). From interfacial ring-opening polymerization to melt processing of cellulose nanowhisker-filled polylactide-based nanocomposites. *Biomacromolecules, 12*(7), 2456–2465.
Habibi, Y., Goffin, A. L., Schiltz, N., Duquesne, E., Dubois, P., & Dufresne, A. (2008). Bionanocomposites based on poly(ε-caprolactone)-grafted cellulose nanocrystals by ring-opening polymerisation. *Journal of Materials Chemistry, 18*(41), 5002–5010.
Habibi, Y., Lucia, L. A., & Rojas, O. J. (2010). Cellulose nanocrystals: Chemistry, self-assembly, and applications. *Chemical Reviews, 110*(6), 3479–3500.
Huan, S., Bai, L., Liu, G., & Han, G. (2015). Electrospun nanofibrous composites of polystyrene and cellulose nanocrystals: Manufacture and characterization. *RSC Advances, 5*(63), 50756–50766.
Jonoobi, M., Harun, J., Mathew, A. P., & Oksman, K. (2010). Mechanical properties of cellulose nanofiber (CNF) reinforced polylactic acid (PLA) prepared by twin screw extrusion. *Composites Science and Technology, 70*(12), 1742–1747.
Jonoobi, M., Mathew, A. P., Abdi, M. M., Makinejad, M. D., & Oksman, K. (2012). A comparison of modified and unmodified cellulose nanofiber reinforced polylactic acid (PLA) prepared by twin screw extrusion. *Journal of Polymers & the Environment, 20*(4), 991–997.
Joy, J., Jose, C., Yu, X., Mathew, L., Thomas, S., & Pilla, S. (2017). The influence of nanocellulosic fiber, extracted from Helicteres isora, on thermal, wetting and viscoelastic properties of poly(butylene succinate) composites. *Cellulose,* 1–11.
Kowalczyk, M., Piorkowska, E., Kulpinski, P., & Pracella, M. (2011). Mechanical and thermal properties of PLA composites with cellulose nanofibers and standard size fibers. *Composites Part A Applied Science & Manufacturing, 42*(10), 1509–1514.
Li, Y. D., Fu, Q. Q., Wang, M., & Zeng, J. B. (2017). Morphology, crystallization and rheological behavior in poly(butylene succinate)/cellulose nanocrystal nanocomposites fabricated by solution coagulation. *Carbohydrate Polymers, 164*, 75–82.
Lin, N., Huang, J., & Dufresne, A. (2012). Preparation, properties and applications of polysaccharide nanocrystals in advanced functional nanomaterials: A review. *Nanoscale, 4*(11), 3274–3294.
Ljungberg, N., Bonini, C., Bortolussi, F., Boisson, C., Heux, L., & Cavaillé, J. Y. (2005). New nanocomposite materials reinforced with cellulose whiskers in atactic polypropylene: Effect of surface and dispersion characteristics. *Biomacromolecules, 6*(5), 2732–2739.
Mariano, M., Kissi, N. E., & Dufresne, A. (2014). Cellulose nanocrystals and related nanocomposites: Review of some properties and challenges. *Journal of Polymer Science Part B Polymer Physics, 52*(12), 791–806.
Morandi, G., Heath, L., & Thielemans, W. (2009). Cellulose nanocrystals grafted with polystyrene chains through surface-initiated atom transfer radical polymerization (SI-ATRP). *Langmuir, 25*(14), 8280–8286.
Pérezcamargo, R. A., Fernándezd'Arlas, B., Cavallo, D., Debuissy, T., Pollet, E., Avérous, L., et al. (2017). Tailoring the structure, morphology, and crystallization of isodimorphic poly(butylene succinate-ran-butylene adipate) random copolymers by changing composition and thermal history. *Macromolecules, 50*(2), 597–608.
Petera, B., Delattre, C., Pierre, G., Wadouachi, A., Elboutachfaiti, R., Engel, E., et al. (2015). Characterization of arabinogalactan-rich mucilage from Cereus triangularis cladodes. *Carbohydrate Polymers, 127*, 372–380.
Pracella, M., Haque, M. U., & Puglia, D. (2014). Morphology and properties tuning of PLA/cellulose nanocrystals bio-nanocomposites by means of reactive functionalization and blending with PVAc. *Polymer, 55*(16), 3720–3728.
Pranger, L., & Tannenbaum, R. (2008). Biobased nanocomposites prepared by *in situ* polymerization of furfuryl alcohol with cellulose whiskers or montmorillonite clay. *Macromolecules, 41*(22), 8682–8687.
Ray, S. S., Okamoto, K., & Okamoto, M. (2003). Structure-property relationship in biodegradable poly(butylene succinate)/layered silicate nanocomposites. *Macromolecules, 36*(7), 2355–2367.
Salmieri, S., Islam, F., Khan, R. A., Hossain, F. M., Ibrahim, H. M. M., Miao, C., et al. (2014). Antimicrobial nanocomposite films made of poly(lactic acid)-cellulose nanocrystals (PLA-CNC) in food applications: Part A—effect of nisin release on the inactivation of Listeria monocytogenes in ham. *Cellulose, 21*(3), 1837–1850.
Sharifian, I. (2011). Conductive and biodegradable polyaniline/starch blends and their composites with polystyrene. *Iranian Polymer Journal, 20*(4), 319–328.
Shimizu, M., Saito, T., & Isogai, A. (2014). Bulky quaternary alkylammonium counterions

enhance the nanodispersibility of 2,2,6,6-tetramethylpiperidine-1-oxyl-oxidized cellulose in diverse solvents. *Biomacromolecules, 15*(5), 1904–1909.
Stroganov, V., Al-Hussein, M., Sommer, J. U., Janke, A., Zakharchenko, S., & Ionov, L. (2015). Reversible thermosensitive biodegradable polymeric actuators based on confined crystallization. *Nano Letters, 15*(3), 1786–1790.
Totaro, G., Sisti, L., Celli, A., Askanian, H., Verney, V., & Leroux, F. (2016). Poly(butylene succinate) bionanocomposites: A novel bio-organo-modified layered double hydroxide for superior mechanical properties. *RSC Advances, 6*(6), 4780–4791.
Trabelsi-Souissi, S., Oturan, N., Bellakhal, N., & Oturan, M. A. (2011). Application of the photo-Fenton process to the mineralization of phthalic anhydride in aqueous medium. *Desalination & Water Treatment, 25*(1–3), 210–215.
Trache, D., Hussin, M. H., Hui, C. C., Sabar, S., Fazita, M. R., Taiwo, O. F., et al. (2016). Microcrystalline cellulose: Isolation, characterization and bio-composites application—a review. *International Journal of Biological Macromolecules, 93*, 789–804.
Trache, D., Hussin, M. H., Haafiz, M. K., & Thakur, V. K. (2017). Recent progress in cellulose nanocrystals: Sources and production. *Nanoscale, 9*(5), 1763–1786.
Wan, C., & Chen, B. (2013). Reinforcement of biodegradable poly(butylene succinate) with low loadings of graphene oxide. *Journal of Applied Polymer Science, 127*(6), 5094–5099.
Xu, C., Chen, J., Wu, D., Chen, Y., Lv, Q., & Wang, M. (2016). Polylactide/acetylated nanocrystalline cellulose composites prepared by a continuous route: A phase interface-property relation study. *Carbohydrate Polymers, 146*, 58–66.
Yu, J., Asai, S., & Sumita, M. (2000). Time-resolved FTIR study of crystallization behavior of melt-crystallized poly(phenylene sulfide). *Journal of Macromolecular Science Part B, 39*(2), 279–296.
Zare, E. N., Lakouraj, M. M., & Mohseni, M. (2014). Biodegradable polypyrrole/dextrin conductive nanocomposite: Synthesis, characterization, antioxidant and antibacterial activity. *Synthetic Metals, 187*(9), 9–16.
Zhang, X., & Zhang, Y. (2015). Poly(butylene succinate-co-butylene adipate)/cellulose nanocrystal composites modified with phthalic anhydride. *Carbohydrate Polymers, 134*(1), 52–59.
Zhang, X., & Zhang, Y. (2016). Reinforcement effect of poly(butylene succinate) (PBS)-grafted cellulose nanocrystal on toughened PBS/polylactic acid blends. *Carbohydrate Polymers, 140*(1), 374–382.
Zhang, N., Yu, A., Liang, A., Zhang, R., Feng, X., & Ding, E. (2013). Preparation of SiC whisker and application in reinforce of polystyrene resin composite materials. *Journal of Applied Polymer Science, 130*(1), 579–586.
Zhang, C., Salick, M. R., Cordie, T. M., Ellingham, T., Dan, Y., & Turng, L. S. (2015). Incorporation of poly(ethylene glycol) grafted cellulose nanocrystals in poly(lactic acid) electrospun nanocomposite fibers as potential scaffolds for bone tissue engineering. *Materials Science & Engineering C Materials for Biological Applications, 49*(39), 463–471.
Zhang, X., Ma, P., & Zhang, Y. (2016). Structure and properties of surface-acetylated cellulose nanocrystal/poly (butylene adipate-co-terephthalate) composites. *Polymer Bulletin, 73*(1), 2073–2085.
Zhou, Y., Fu, S., Zhang, L., Zhan, H., & Levit, M. V. (2014). Use of carboxylated cellulose nanofibrils-filled magnetic chitosan hydrogel beads as adsorbents for Pb(II). *Carbohydrate Polymers, 101*(1), 75–82.